Alternating droplet generation and controlled dynamic droplet fusion in microfluidic device for CdS nanoparticle synthesis†

Lung-Hsin Hung,[a] Kyung M. Choi,[b] Wei-Yu Tseng,[a] Yung-Chieh Tan,[c] Kenneth J. Shea[b] and Abraham Phillip Lee*[cd]

Received 30th September 2005, Accepted 6th December 2005
First published as an Advance Article on the web 5th January 2006
DOI: 10.1039/b513908b

A multifunctional and high-efficiency microfluidic device for droplet generation and fusion is presented. Through unique design of the micro-channels, the device is able to alternately generate droplets, generating droplet ratios ranging from 1 : 5 to 5 : 1, and fuse droplets, enabling precise chemical reactions in several picoliters on a single chip. The controlled fusion is managed by passive control based on the channel geometry and liquid phase flow. The synthesis of CdS nanoparticles utilizing each fused droplet as a microreactor for rapid and efficient mixing of reagents is demonstrated in this paper. Following alternating droplet generation, the channel geometry allows the exclusive fusion of alternate droplets with concomitant rapid mixing and produces supersaturated solution of $Cd^{2+}$and S^{2-} ions to form CdS nanoparticles in each fused droplet. The spectroscopic properties of the CdS nanoparticles produced by this method are compared with CdS prepared by bulk mixing.

Introduction

The use of microfluidics offers a number of advantages over conventional flow control technology.[1–3] High surface-to-volume ratio and small volume expedite the chemical reaction in microfluidic devices and improve the product yield. Microfluidic devices offer the capability of automated multi-step biochemical analysis and reactions. The overall goal of micro total analysis systems is to carry out all operations, normally performed in the laboratory including synthesis, processing, purification, and analysis on one microfluidic device efficiently and economically by using minute amounts of solvents and reagents.

Microfluidic droplet techniques have been widely developed recently[4–9] and provide an approach to improve mixing efficiency and better control concentrations of reagents; which are difficult in laminar flow-dominant microfluidic devices where fluid mixing is limited by diffusion. The diffusion driven mixing is slow and the parabolic flow profile causes dispersion in size and other crucial parameters. Laminar flow mixing prior to droplet generation and electro-wetting are alternative methods to controlling and mixing chemicals,[10–11] while the first approach has local instability caused by the pinching of droplets[12] and asymmetric shear force may compromise the precise control of reagent composition in each droplet; electrowetting requires extra instruments and could absorb bio-molecules on the wetting surface.

Micro-sized droplets contain an equal concentration of reagents and fusion of droplets with different reagents would allow rapid chemical synthesis and in constant volume. Ismagilov, Higuchi, Fielden *et al.* and our group have shown similar interests in alternating droplet generation,[5,11,13–14] which means droplets are generated from two liquid inlets alternately. The concepts to fuse droplets were shown previously,[4,10] while the fusion of different sizes of droplets requires the larger drop to precede the smaller one. However, controlled droplet fusion, especially for same-sized droplet fusion, is still a challenge, mostly because of the difficulty to manipulate droplets under high flow velocity. Without same-sized droplet fusion, extra calculation is required to control and determine the mixing amount and/or concentration of reagents. Here we present a microfluidic device manipulating droplets by the geometry of channels (alternating droplets and the generation of velocity gradients) and the control of flow rates of liquids. As a result no external force (ex. electrical, magnetic field, heat) is required. The device has the advantages of producing uniform droplet sizes, rapid mixing, alternating droplet generation, adjustable droplet generation ratio and controlled droplet fusion for sample combinations.[15]

Microfluidic devices have been used for synthesis of both organics and inorganics. Recently several groups have reported microfluidic strategies for the synthesis of semiconductor nanoparticles.[16–19] Here we also carry out the synthesis of CdS nanoparticles as a demonstration of the microfluidic droplet fusion approach.

[a]*Department of Chemical Engineering and Materials Science, University of California at Irvine, Irvine, CA 92697, USA*
[b]*Department of Chemistry, University of California at Irvine, Irvine, CA 92697, USA*
[c]*Department of Biomedical Engineering, 204 Rockwell Engineering Center, University of California at Irvine, Irvine, CA 92697, USA. E-mail: aplee@uci.edu*
[d]*Department of Mechanical and Aerospace Engineering, University of California at Irvine, Irvine, CA 92697, USA*

† Electronic supplementary information (ESI) available: Droplet size *vs.* pinch junction width. See DOI: 10.1039/b513908b

Experimental

Design of microfludic fusion channel

The innovation of the present work arises from a microfluidic approach for rapid mixing and consequent chemical reactions. The schematic of microfluidic channel pattern is shown in Fig. 1 and 2. The device is comprised of three inlets, a double-T junction, a tapered chamber, and a switchback outlet channel. Three inlet channels are joined at a double-T junction that opens to a tapered expansion chamber. This tapered chamber is used to induce velocity gradient for the droplets to contact and fuse. A 60 μm-wide switchback outlet channel is connected to the tapered chamber for droplet collection and product analysis. The two triangular wings between the inlets and the T-junction have the function to reduce the flow instability and prevent reagents from back flowing.

Microfabrication

A PDMS stamp with the microfluidic channel pattern is cast with a SU-8 mold. The surface of the PDMS is subjected to air plasma then directly bonded to a glass slide. The interior surface of the inner channels (both PDMS and glass) is treated with tridecafluoro-tetrahydrooctyl-trichlorosilane to make it hydrophobic. Silicon oil is used as a carrier fluid and two water inlets are used as dispersed phases. Each of three liquid phases is injected into the microchannel and controlled by a syringe pump respectively.

At the double-T junction (Fig. 2), two water phases are sheared by the silicon oil stream and monodispersed droplets are generated alternatively and synchronously. Generated droplets are aligned in the tapered chamber before fusion and exiting to the outlet channel. The system is designed so as to create an alternation in droplet generation as well as controlled droplet fusion. A high speed camera with frame rates up to 10 000 frames s^{-1} (Photron Ltd.) is used to record droplet generation and fusion. Droplet size is estimated using Scion Image program (Scion Co.).

CdS nanoparticle synthesis and analysis

CdS nanoparticles synthesis and analysis utilizing this microfluidic device is designed and demonstrated. Each fused droplet acts as a micro-reactor for reagent combination and reaction. Two reagent streams, 1×10^{-4} M of $Cd(NO_3)_2{\cdot}4H_2O$ and $NaS{\cdot}9H_2O$, replace previous water inlets.

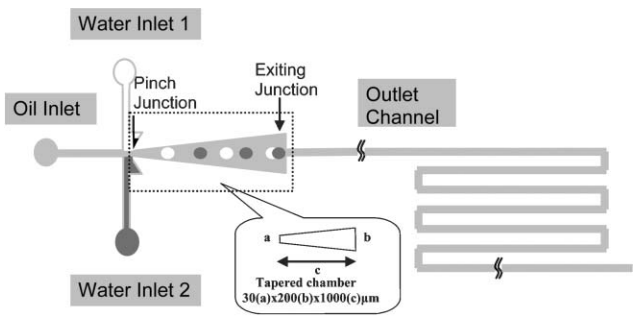

Fig. 1 Schematic diagram of the microchannel pattern. The dimension of the tapered chamber is shown as $a \times b \times c$.

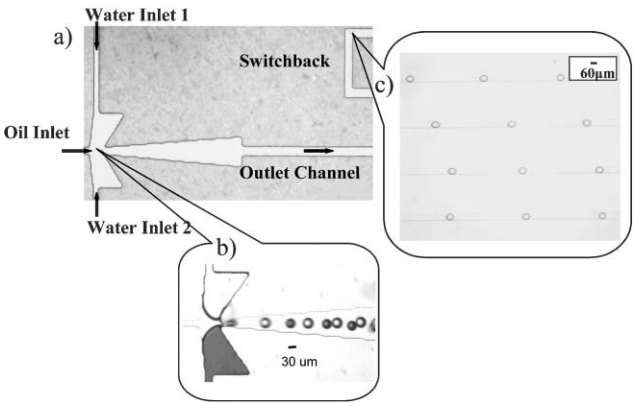

Fig. 2 (a) Microscopic image of the PDMS channel magnified at the double-T junction channel. (b) Water-in-oil alternating microdroplet generation. Green dye is added into water inlet 2 for the differentiation purpose. (c) Fused droplets align in the long switchback channel.

$Cd(NO_3)_2{\cdot}4H_2O$ solution contains sodium polyphosphate as the stabilizer.

The concentration of each inlet solution is accurately prepared and the exact volume of each droplet is achieved by the ability to generate monodispersed droplets.[4] Following alternating droplet generation the taper geometry results in exclusive fusion of alternate droplets with concomitant rapid mixing of their contents to produce a supersaturated solution of Cd^{2+} and S^{2-} ions. CdS nanoparticle formation takes place as the individual fused droplet traverses the long switchback channel. Fig. 2(c) shows an alignment of CdS-containing droplets in the outlet channel. The distance between each droplet is approximately 0.7 mm. Precipitation of CdS nanoparticles ensues under these controlled conditions and each fused droplet is isolated by carrier fluid to prevent further aggregation. The outlet is linked to a quartz flow cell (10 mm path length) to collect the CdS particles for spectroscopic characterization and AFM imaging.

Results and discussion

Synchronized alternating droplet generation

To verify alternating droplet formation and exclusive pair-wise droplet fusion, a green dye-containing aqueous solution is used to differentiate the two aqueous streams. The microscopic image of droplet production in Fig. 2(b) reveals the alternation.

The alternating droplet generation is the result of a ''push–pull'' mechanism. At the double-T junction, two water phases compete to pass through. When water stream 1 is generating a droplet, water stream 2 is being pushed as pressure builds up. This build-up pressure forces water stream 2 into the pinch junction to generate the next droplet. Utilizing this push–pull mechanism, alternating droplet generations can be achieved over a wide range of droplet ratios, droplet generation rates, and droplet sizes. Fig. 3 shows different droplet ratios based on the pressure built-up of each stream at the double-T junction. The push–pull mechanism between two reagent streams results in synchronized alternating droplet generation and adjustable droplet generation ratio. By adjusting the

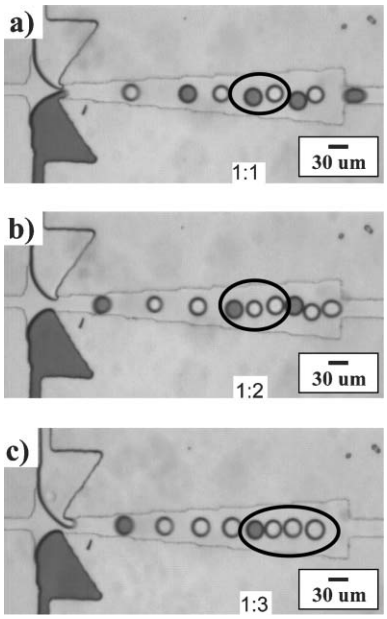

Fig. 3 Droplet ratio control by adjusting inlet flow rates (a) 1 : 1, (b) 1 : 2, (c) 1 : 3.

relative flow rates in the two reagent inlet channels, the device allows continuous alternating droplet formation with droplet ratios from 1 : 5 to 5 : 1. Beyond these ratios, the large pressure difference between two water inlets will result in unstable droplet generation. The specific flow rate range applicable for specific droplet generation ratios is shown in Fig. 4. The ability to control droplet ratio provides different mixing ratio and concentration control for chemical and drug synthesis applications.

Droplet size is mainly controlled by the pinch junction width *a* (as shown in Fig. 1), where three inlet channels merge (see ESI†). At constant silicon oil flow rate, the wider T-junction results in larger droplets while two aqueous flow rates only affect droplet size slightly, therefore a minor change of inlet flow rates wouldn't affect the droplet size.

The pair-droplet generation frequency acts as a function of the flow rates between two immiscible phases (Fig. 5). Both higher oil and water flow rates result in higher droplet generation frequency ranging from 20–840 pairs s^{-1}. The

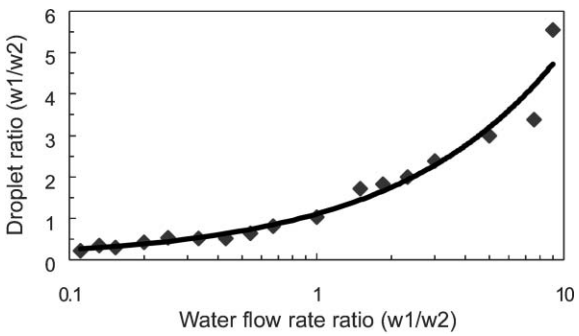

Fig. 4 Droplet ratio increases as relative two stream flow rate ratio increases. The droplet ratio of two streams is adjustable from 1 : 5 to 5 : 1.

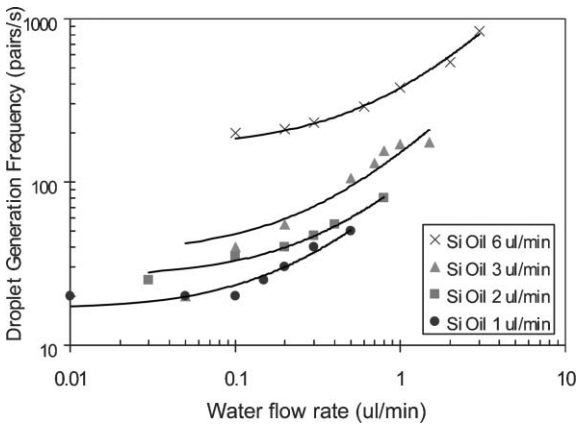

Fig. 5 Pair-droplet generation frequency acts as the function of oil and water flow rates.

higher oil flow rate, the higher offset of water flow rate is required for the pressure built-up in the pinch junction for droplet generation. As mentioned before, the droplet size is mainly controlled by the width of pinch junction, so the droplet size remains constant while generation frequency is changed, which is another advantage that can be utilized.

Droplet fusion

Mixing of the reagent streams is accomplished by selectively fusing the alternating reagent droplets. Chesters[20] described the droplet coalescence mechanism with three steps. The first step is particle collision. The second step is film drainage during droplet collisions. The third step is film rupture resulting in droplet coalescence. Based on this concept, the tapered chamber is designed to generate velocity gradient and allow droplet approaching and oil film drainage between droplets. The channel width reduction between the tapered channel and outlet channel increases the flow pressure to prompt the film rupture and facilitate the droplet fusion. Both surface tension driven mixing and picoliter droplet volume expedite the mixing speed and efficiency. This facilitates the chemical reaction taking place in each fused droplet and prevents aggregation. Therefore nanoparticles and small reactant size distributions are possible to be achieved.

Since the droplet generation frequency is mainly controlled by the flow rates of the two immiscible phases, the distance between binary droplets is adjustable and precise binary collisions can be accomplished in the tapered chamber. The dye-containing aqueous stream differentiates the two droplets allowing visualization of droplet fusion and mixing. Gratifyingly, the device demonstrated a high accuracy for fusion of adjacent droplets (Fig. 6). Under different oil and water flow rate combinations, the phase diagram of droplet fusion is mapped in Fig. 7. In phase I, each droplet pair collide and fuse before entering the outlet channel. In phase II, the excessive water flow rate results in instability and random fusion of multiple droplets. In phase III no droplet fusion occurs, this is due to either the droplet generation frequency being too low for droplets to collide or the high flow rates reducing the contact time for droplets to fuse. The size distribution of the fused droplets is within 3% range while this

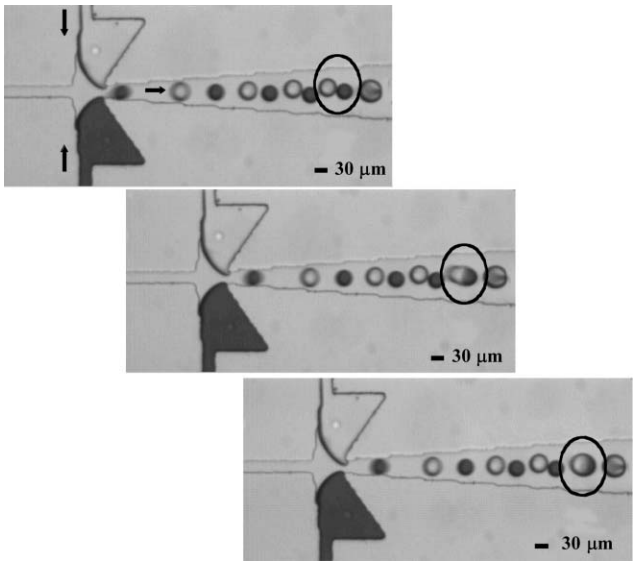

Fig. 6 Dynamic fusion of alternating droplets.

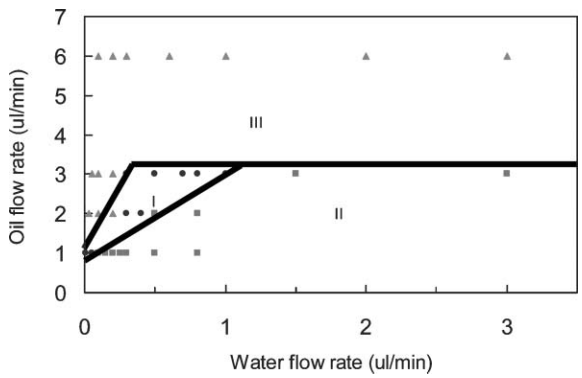

Fig. 7 The phase diagram depicting the relationship between the droplet fusion and oil, water flow rates: pair droplet fusion (phase I—circle), random droplet coalescence (phase II—square), and no droplet fusion (phase III—triangle).

could be as large as 50% for random droplet coalescence. The flow rate in phase I is the ideal condition to operate droplet fusion; while phase III can be utilized for alternating droplet collection and sorting purposes.

For the demonstration of CdS nanoparticle synthesis, the merging of two reagents is achieved in each fused droplet containing supersaturated solutions of Cd^{+2} and S^{-2} ions. The final concentration of Cd^{2+}/S^{2-} in each droplet is 5×10^{-5} M.

Spectroscopic characterizations

Upon droplet generation and subsequent fusion of the two reagent solutions, fused droplets enter the 60 μm switchback channel. The sizes of the CdS particles formed in each droplet depend in part on concentrations of reagent solutions, the final degree of supersaturation, and the speed of mixing.

A microscopic image of isolated CdS-containing droplets align in the 60 μm switchback channel is shown in Fig. 2(c), and an AFM image of CdS nanoparticles prepared by microfluidic droplet fusion approach is shown in Fig. 8. The CdS nanoparticle-containing droplets are collected and analyzed by absorption and fluorescence spectroscopy (Fig. 9 and 10). The CdS particle size is calculated using Brus' equation.[21]

Fig. 9 shows absorptions of CdS particles prepared by both microfluidic droplet fusion and bulk mixing. The narrower size distribution of CdS absorption resulted when reagents are mixed using the microfluidic device. Additionally, CdS

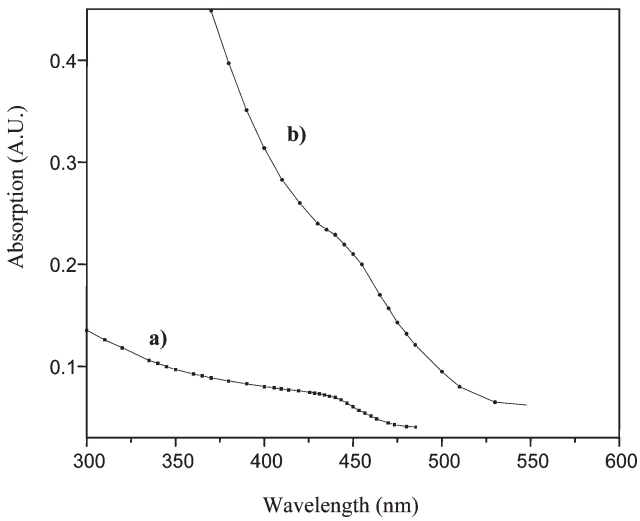

Fig. 9 UV absorption bands of CdS particles prepared by (a) microfluidic droplet fusion and (b) direct mixing.

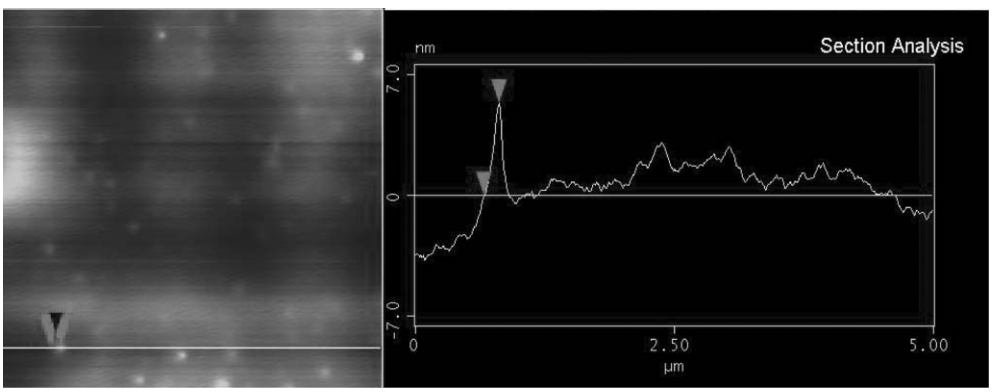

Fig. 8 AFM image of CdS nanoparticles prepared by microfludic droplet fusion approach.

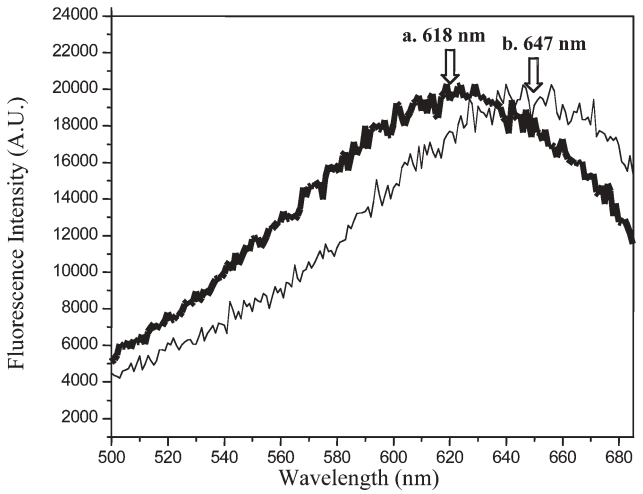

Fig. 10 Fluorescence emissions of CdS particles prepared by (a) microfluidic mixing—thick solid line and (b) direct mixing—dashed solid line; the emissions are obtained at 400 nm excitation.

particles prepared by microfluidic droplet fusion show better chemical stability and less aggregation after mixing.

From the absorption spectra in Fig. 9, CdS prepared by microfludic fusion ranged from 477 (2.6 eV ≡ 8.2 nm CdS in diameter) to 427 nm (2.9 eV ≡ 4.2 nm CdS in diameter). A comparison of the fluorescence emission of the CdS between microfludic fusion and bulk mixing is given in Fig. 10; the emissions are obtained at 400 nm excitation.

As shown in Fig. 10, the emission maximum of CdS particles prepared by microfluidic mixing is approximately 618 nm. The overlaid spectra reveal that particles prepared by microfluidic droplet fusion have blue shifted (618 *vs*. 647 nm) and indicate a smaller average particle size arising from this method of preparation. Comparison of the UV absorption spectra shown in Fig. 9 is also consistent with this result shown in Fig. 10. These comparisons of materials prepared by the microfluidic approach with direct "conventional" approaches highlight the potential advantages of microreactors.

Conclusions

The described microfluidic device demonstrates the ability to synchronize the generation of binary droplets in different sizes, ratios, frequencies, and the capibility of fusing droplets under various flow rate ranges. The micro droplet-reactors permit the controlled synthesis of photoluminescent CdS nanoparticles. The CdS absorption and fluorescence are blue shifted when compared with particles prepared by bulk mixing. The ability of the micro device to post-process the synthesized CdS nanoparticles is an additional advantage. Furthermore, parallel microchannels and multiplexing will permit the synthesis of multigram quantities.

Acknowledgements

We would like to acknowledge Rita Kuo for experimental data analysis.

References

1 K. Jensen and A. P. Lee, *Lab Chip*, 2004, **4**, 31N–32N.
2 S. J. Haswell, R. J. Middleton, B. O'Sullivan, V. Skelton, P. Watts and P. Styring, *Chem. Commun.*, 2001, **5**, 391–398.
3 D. R. Reyes, D. Lossifidis, P.-A. Auroux and A. Manz, *Anal. Chem.*, 2002, **74**, 2623–2636.
4 Y. C. Tan, J. S. Fisher, A. I. V. Lee, V. Cristini and A. P. Lee, *Lab Chip*, 2004, **4**, 292–298.
5 B. Zheng, J. D. Tice and R. F. Ismagilov, *Anal. Chem.*, 2004, **76**, 4977–4982.
6 T. Nisisako, T. Torii and T. Higuchi, *Lab Chip*, 2002, **2**, 24–26.
7 T. Thorsen, R. W. Roberts, F. H. Arnold and S. R. Quake, *Phys. Rev. Lett.*, 2001, **86**, 4163–4166.
8 S. L. Anna, N. Bontoux and H. A. Stone, *Phys. Lett.*, 2003, **82**, 364–366.
9 M. He, J. S. Edgar, G. D. M. Jeffries, R. M. Lorenz, J. P. Shelby and D. T. Chiu, *Anal. Chem.*, 2005, **77**, 1539–1544.
10 H. Song, J. D. Tice and R. F. Ismagilov, *Angew. Chem., Int. Ed.*, 2003, **42**, 768–772.
11 A. Macaskill, P. R. Fielden, N. J. Goddard, S. Mohr and B. J. T. Brown, *Proc. MicroTAS 2004*, 2004, **1**, 207–209.
12 W. C. Chao, J. Collins, M. Bachman, G. P. Li and A. P. Lee, *Solid-State Sensor, Actuator and Microsystems Workshop*, 2004, 382–383.
13 L.-H. Hung, W.-Y. Tseng, K. Choi, Y.-C. Tan, K. J. Shea and A. P. Lee, *Proc. MicroTAS 2004*, 2004, **2**, 539–541.
14 S. Okushima, T. Nisisako, T. Torii and T. Higuchi, *Proc. MicroTAS 2004*, 2004, **1**, 258–260.
15 Y.-C. Tan, V. Cristini and A. P. Lee, *Sens. Actuators, B*, 2005, DOI: 10.1016/j.snb.2005.06.008.
16 C. H. Fisher and M. Giersig, *Langmuir*, 1992, **8**, 1475–1478.
17 E. M. Chan, R. M. Mathies and A. P. Alivisatos, *Nano Lett.*, 2003, **3**, 199–202.
18 J. B. Edel, R. Fortt, J. C. DeMello and A. J. DeMello, *Chem. Commun.*, 2002, **10**, 1136–1137.
19 I. Shestopalov, J. D. Tice and R. F. Ismagilov, *Lab Chip*, 2004, **4**, 316–321.
20 A. K. Chesters, *Trans. Inst. Chem. Eng.*, 1991, **69**, 259–270.
21 P. E. Lippens and M. Lannoo, *Phys. Rev. B*, 1989, **39**, 10935–10942; E_g (bulk-CdS) = 2.58 eV, m_e^* (CdS) = 0.19, m_h^* (CdS) = 0.8.

